

# Up-down wavefield retrieval in boreholes using single-component data

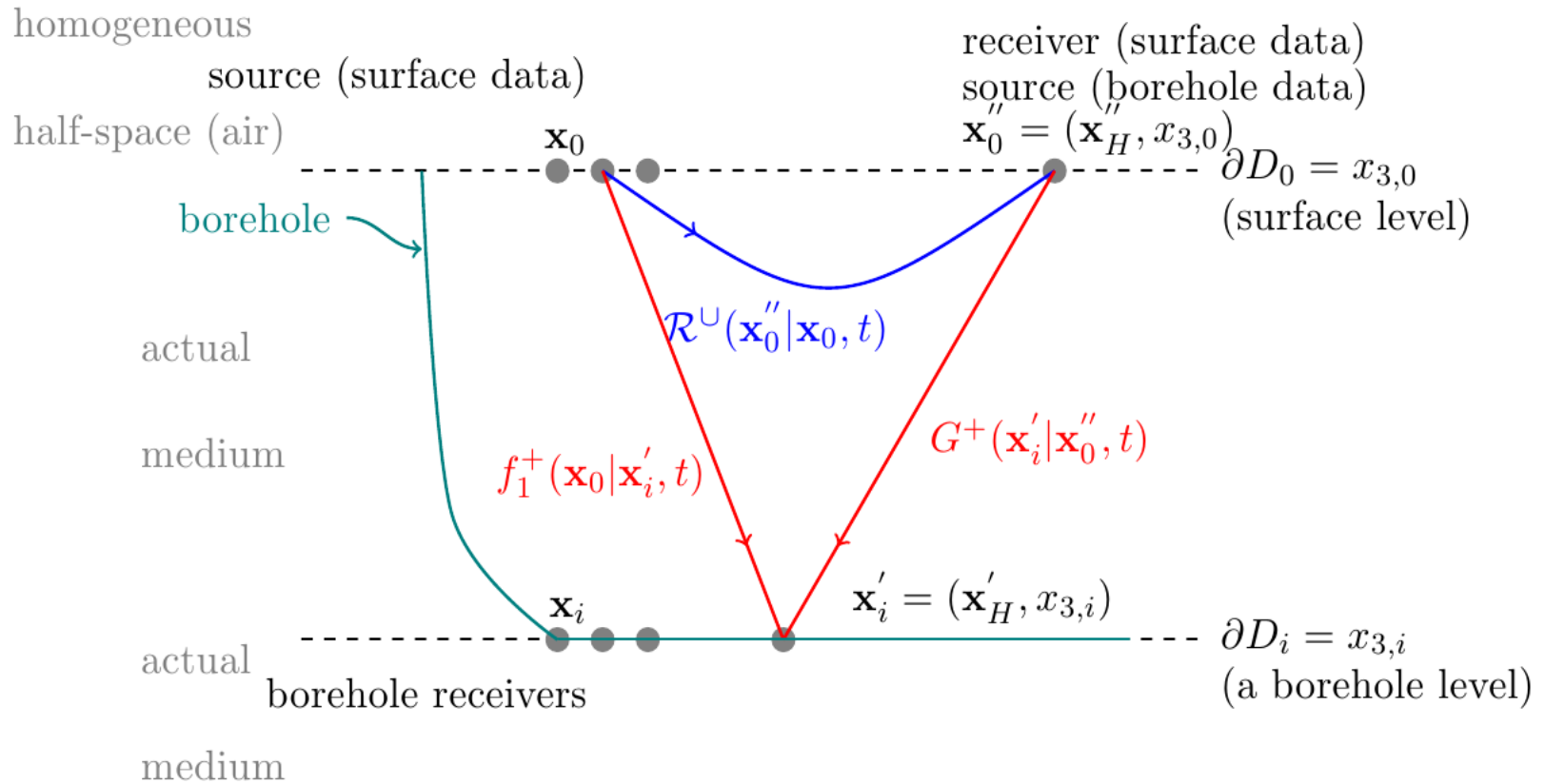
Yi Liu

- Introduction
- Method
- Examples
- Conclusions

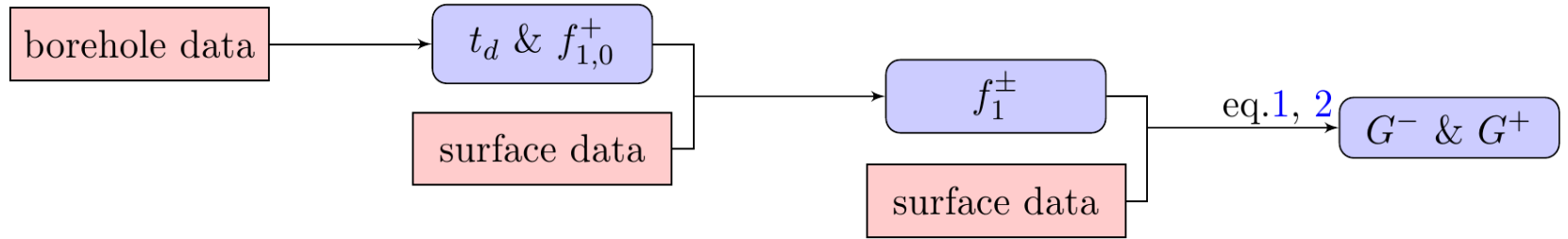
# Introduction

- Different apparent velocity: f-k filter (Embree et al., 1963, Treitel et al., 1967), median filter (Stewart, 1985), tau-p domain separation (Moon et al., 1986), ...
- Wave-equation based using multi-component data: PZ summation (Barr and Sanders, 1989), angle-dependent decomposition (Amundsen and Reitan, 1995)
- Wave-equation based using single-component data: retrieve from surface reflection data

# Introduction



# Method



$$t \geq t_d(\mathbf{x}_0'' | \mathbf{x}_i')$$

$$G^-(\mathbf{x}_i' | \mathbf{x}_0'', t) = \int_{\partial D_0} \int_{-\infty}^t \mathcal{R}^U(\mathbf{x}_0'' | \mathbf{x}_0, t - t') f_1^+(\mathbf{x}_0 | \mathbf{x}_i', t') dt' d\mathbf{x}_0 \quad (1)$$

$$G^+(\mathbf{x}_i' | \mathbf{x}_0'', t) = f_{1,0}^+(\mathbf{x}_0'' | \mathbf{x}_i', -t) - \int_{\partial D_0} \int_{-\infty}^t \mathcal{R}^U(\mathbf{x}_0'' | \mathbf{x}_0, t - t') f_1^-(\mathbf{x}_0 | \mathbf{x}_i', -t') dt' d\mathbf{x}_0. \quad (2)$$

To find  $f_1^+$  :

$$f_{1,k}^+(\mathbf{x}_0''|\mathbf{x}'_i, t) = f_{1,0}^+(\mathbf{x}_0''|\mathbf{x}'_i, t) + \theta(t + t_d(\mathbf{x}_0''|\mathbf{x}'_i)) \int_{\partial D_0} \int_{-\infty}^{\infty} \mathcal{R}^{\cup}(\mathbf{x}_0''|\mathbf{x}'_0, t') f_{1,k-1}^-(\mathbf{x}'_0|\mathbf{x}'_i, t+t') dt' d\mathbf{x}'_0, \quad (3)$$

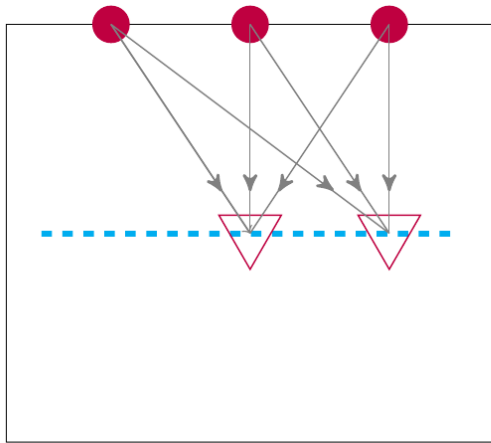
$$f_{1,k}^-(\mathbf{x}_0''|\mathbf{x}'_i, t) = \theta(t_d(\mathbf{x}_0''|\mathbf{x}'_i) - t) \int_{\partial D_0} \int_{-\infty}^{\infty} \mathcal{R}^{\cup}(\mathbf{x}_0''|\mathbf{x}'_0, t - t') f_{1,k}^+(\mathbf{x}'_0|\mathbf{x}'_i, t') dt' d\mathbf{x}'_0, \quad (4)$$

with

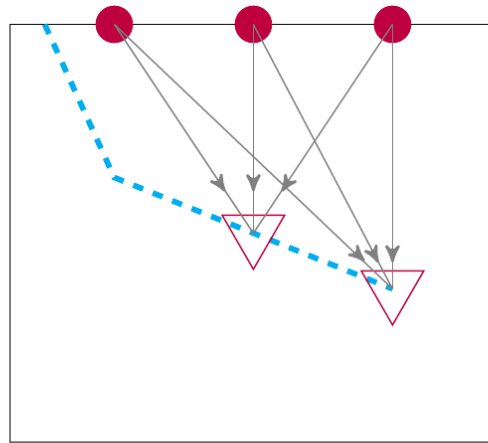
$$f_{1,0}^+(\mathbf{x}_0''|\mathbf{x}'_i, t) \approx G_d(\mathbf{x}'_i|\mathbf{x}_0'', -t), \quad (5)$$

(Rose, 2002; Brogгинi et al., 2012, ...)

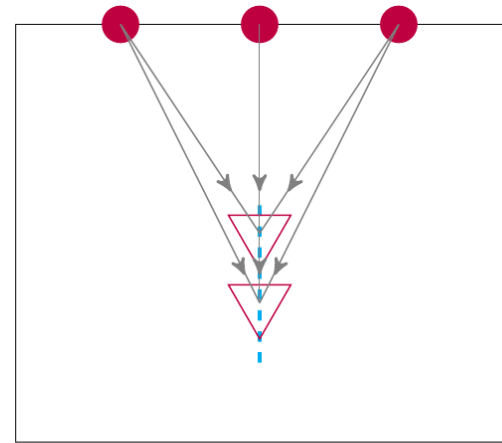
# Method



a)

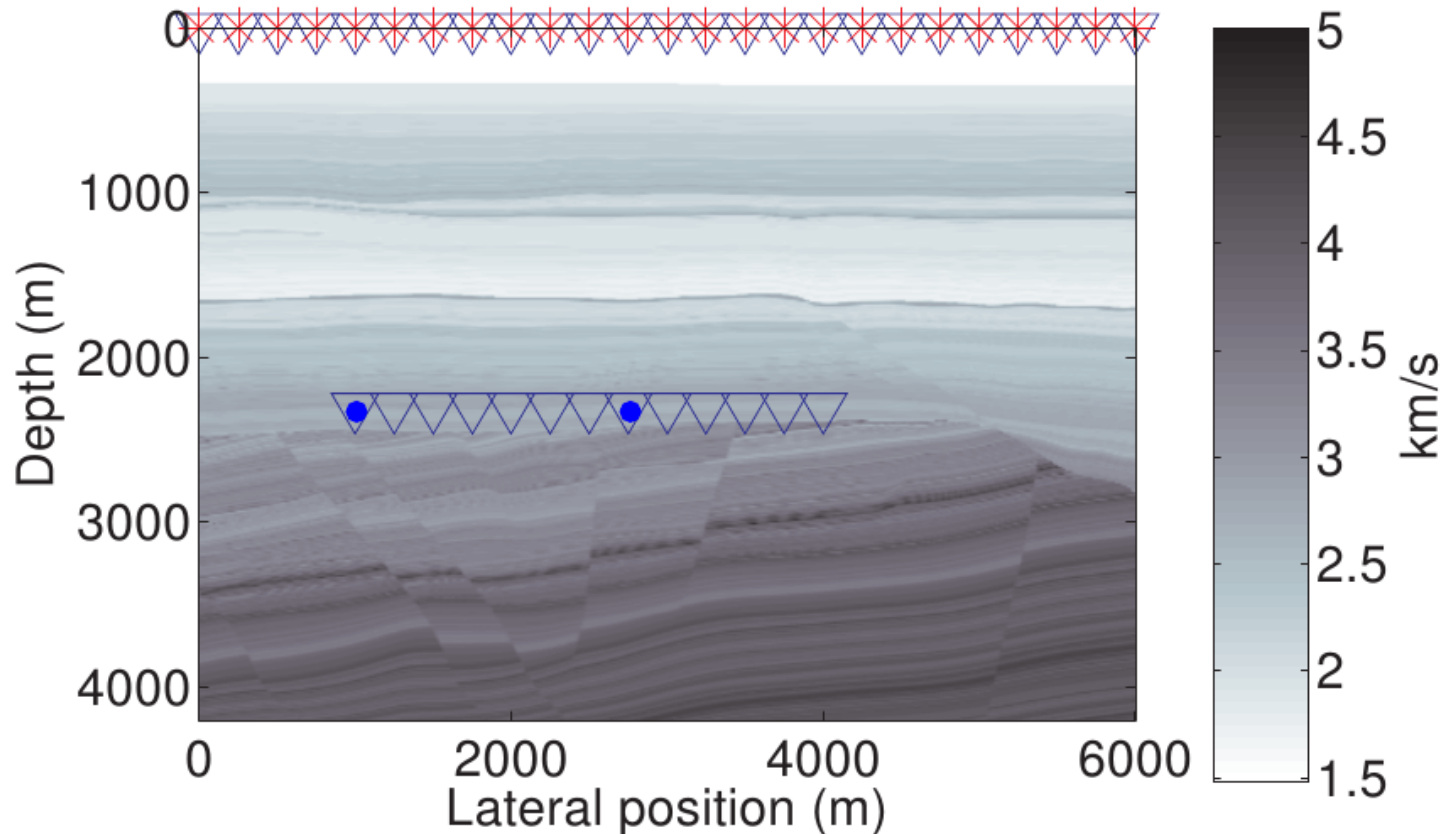


b)



c)

# Example 1: horizontal case

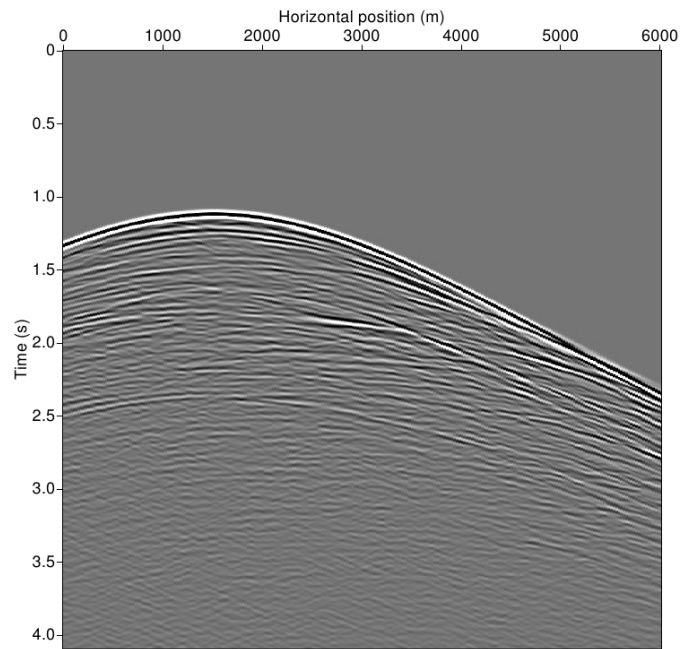


Surface:  $n_{src} = n_{rcv} = 241$ ;  $d_{src} = d_{rcv} = 25$  m;  $f_{max} = 55$  Hz.

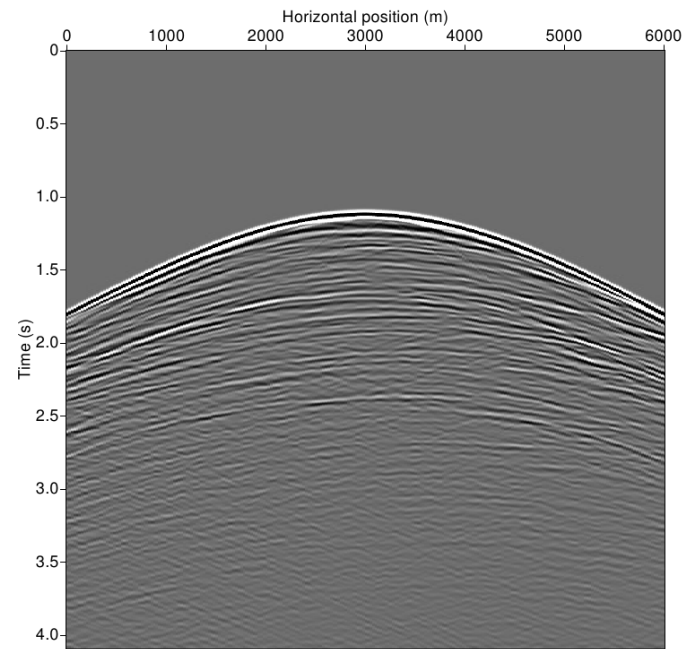
Borehole:  $n_{rcv} = 129$ ;  $d_{rcv} = 25$  m;  $z_{rcv} = 2300$  m; Ricker, 15 Hz.



# Example 1: common-receiver gather, borehole data

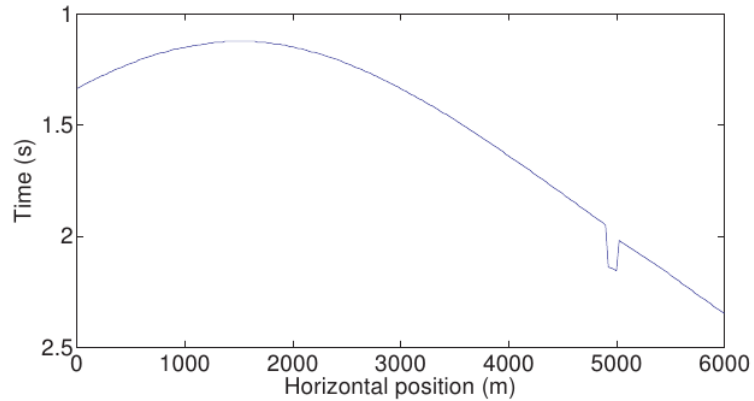


a)

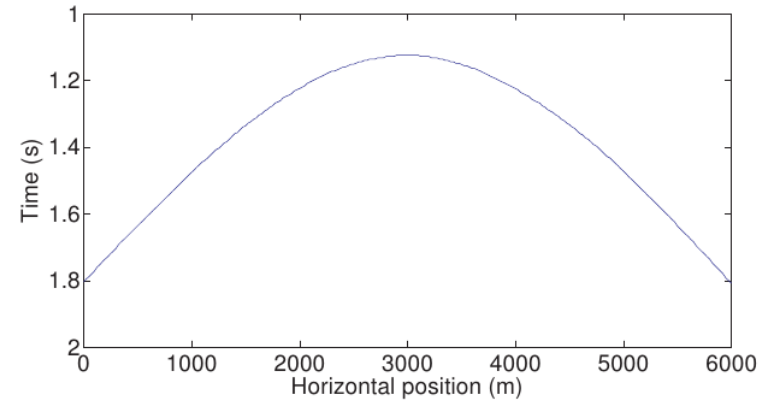


b)

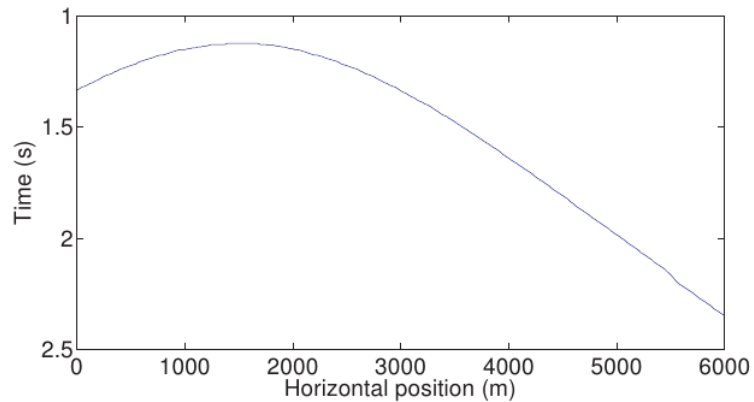
# Example 1: direct arrivals' traveltime curves



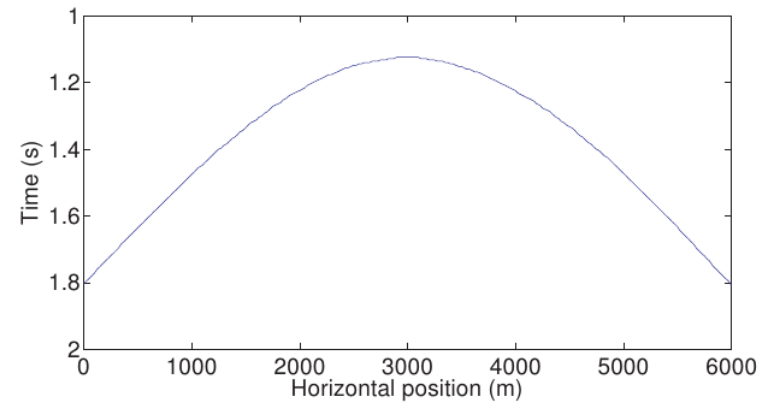
a)



b)

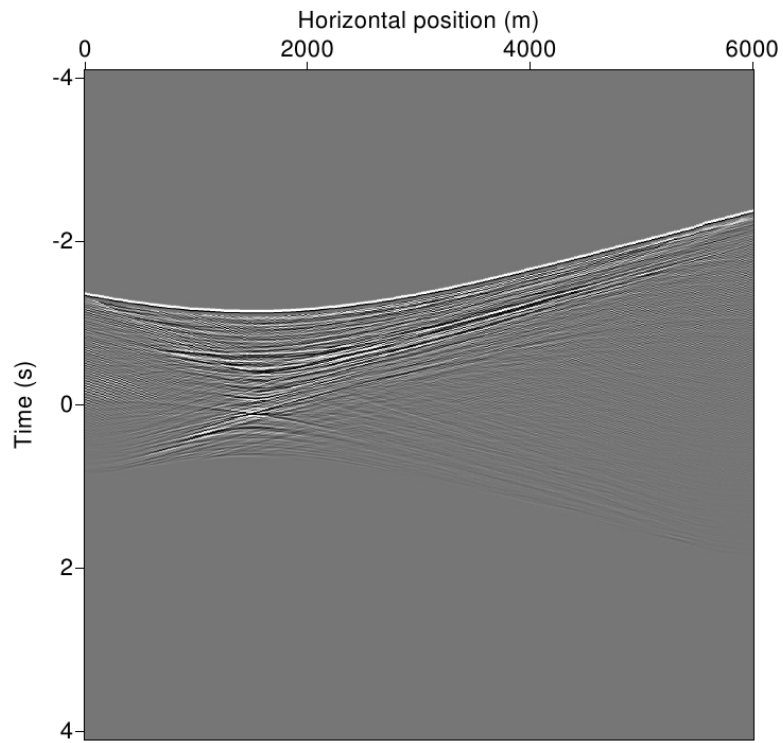


c)

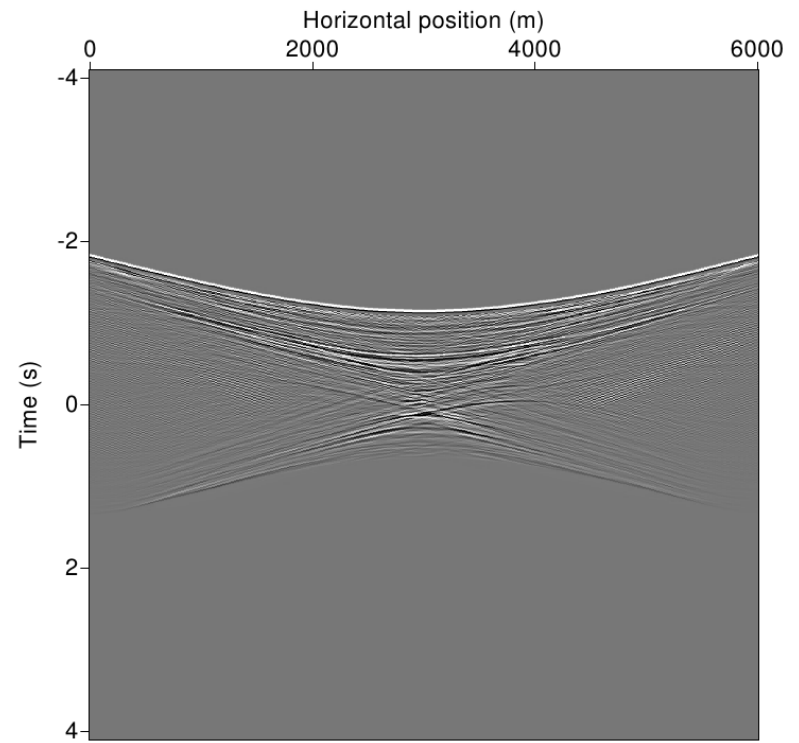


d)

# Example 1: computed focusing functions $f_1^+$

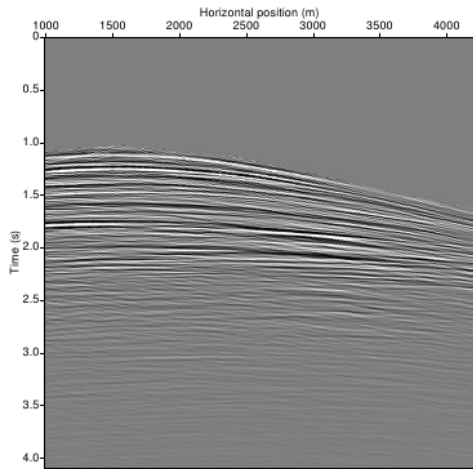


a)

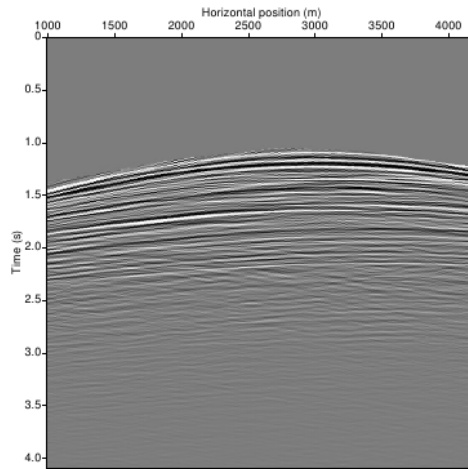


b)

# Example 1: comparison of the upgoing wavefields

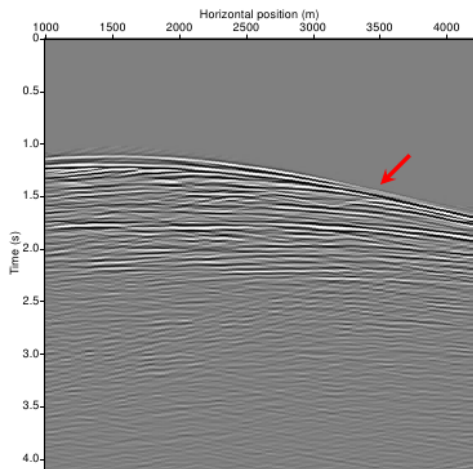


a)

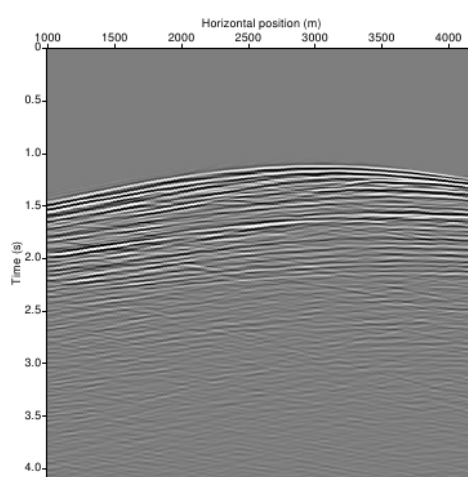


b)

single-component



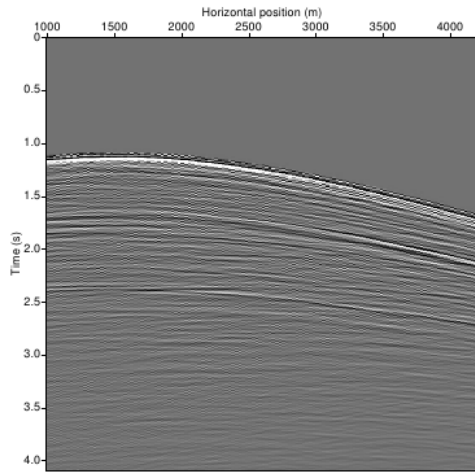
c)



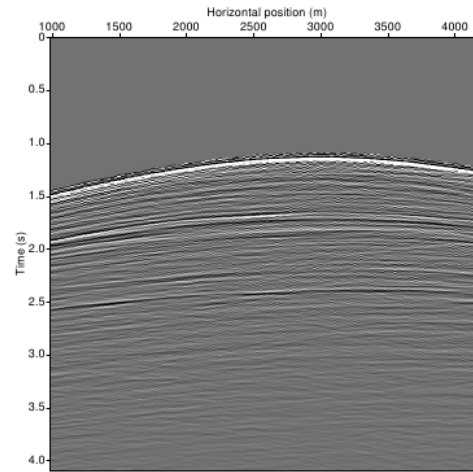
d)

multi-component

# Example 1: comparison of the downgoing wavefields

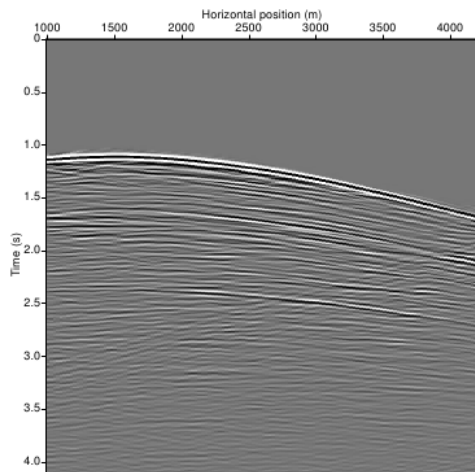


a)

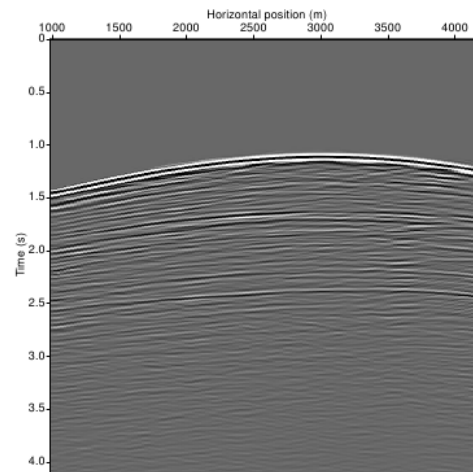


b)

single-component



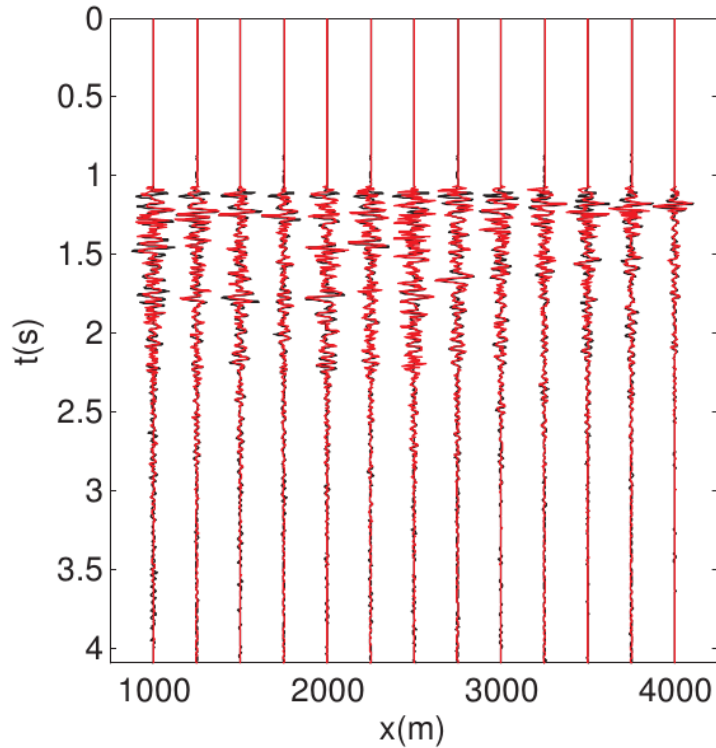
c)



d)

multi-component

# Example 1: comparison of the zero-offset

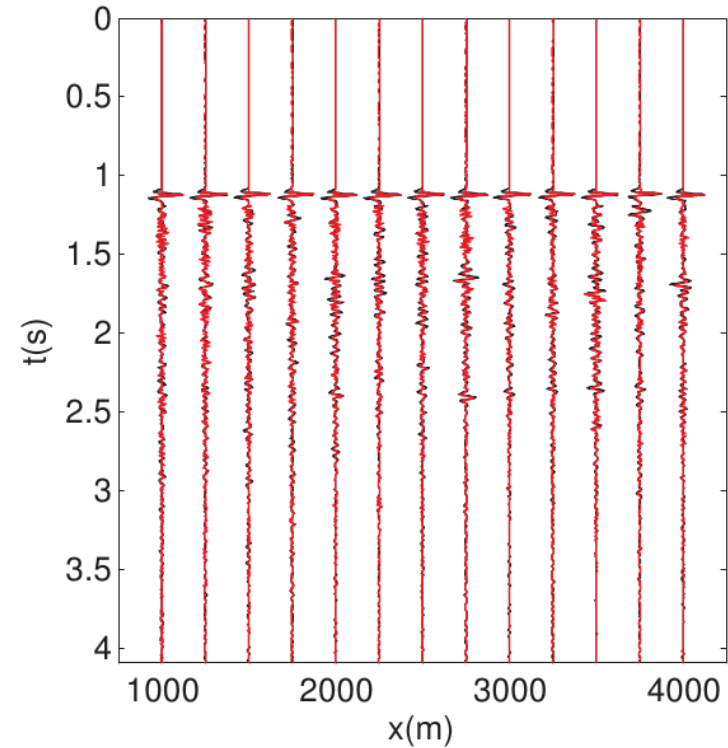


a)

a) The upgoing wavefield

red: the single-component approach

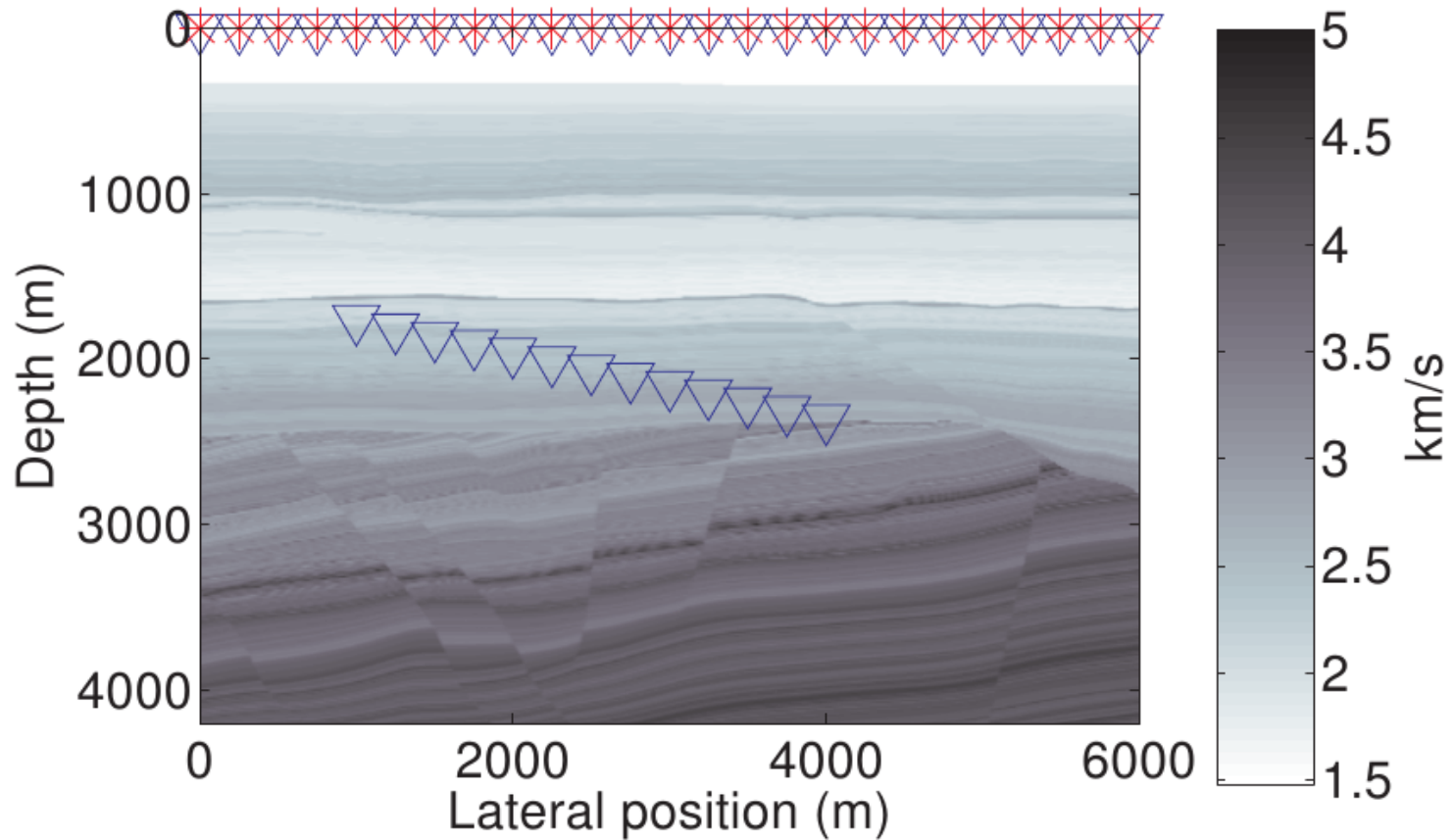
black: standard multi-component approach (p and vz).



b)

b) The downgoing wavefield

## Example 2: deviated borehole

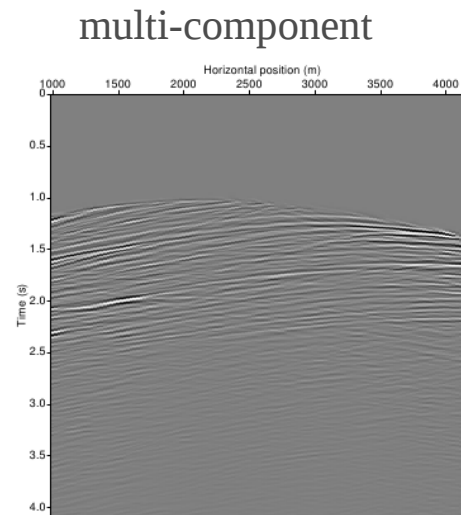
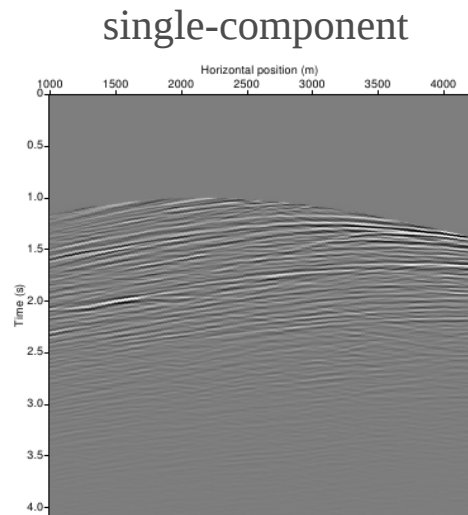


Surface:  $n_{src} = n_{rcv} = 241$ ;  $d_{src} = d_{rcv} = 25$  m;  $f_{max} = 55$  Hz.

Borehole:  $n_{rcv} = 129$ ;  $d_{xrcv} = 25$  m;  $d_{zrcv} = 5$  m;  $z_{rcv} = [1760, 2400]$  m; Ricker, 15 Hz.

# Example 2: comparison of the up-down wavefields

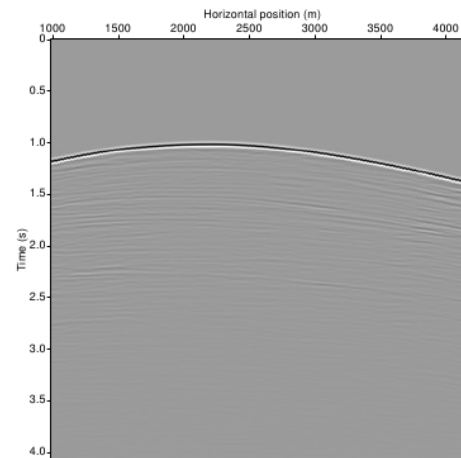
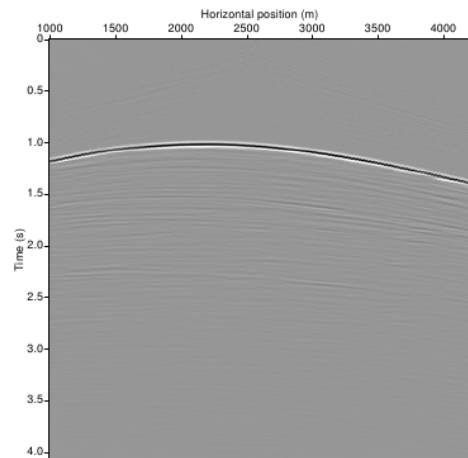
Upgoing



a)

b)

Downgoing

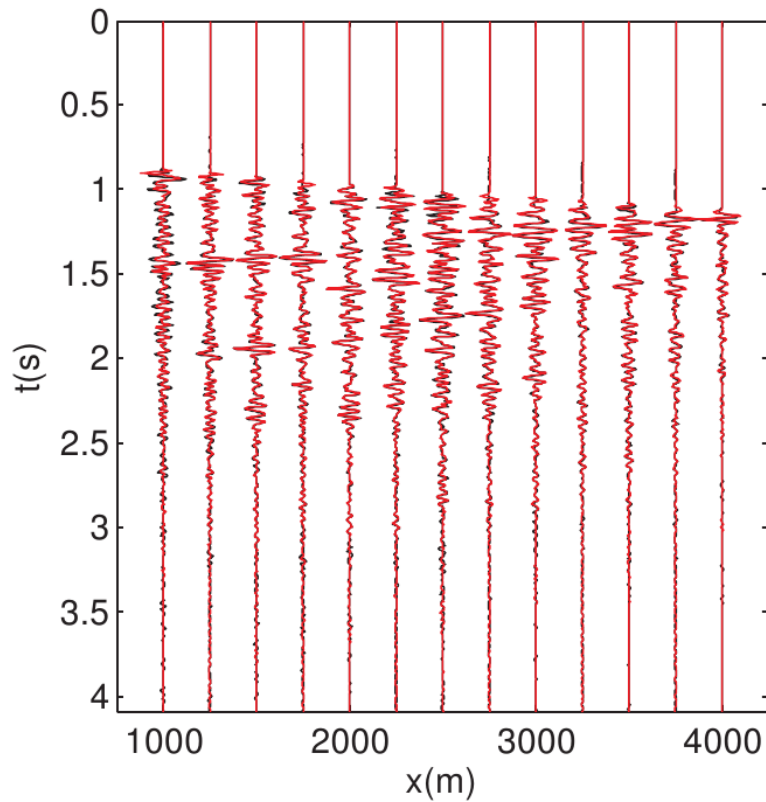


c)

d)



## Example 2: comparison of the zero-offset result

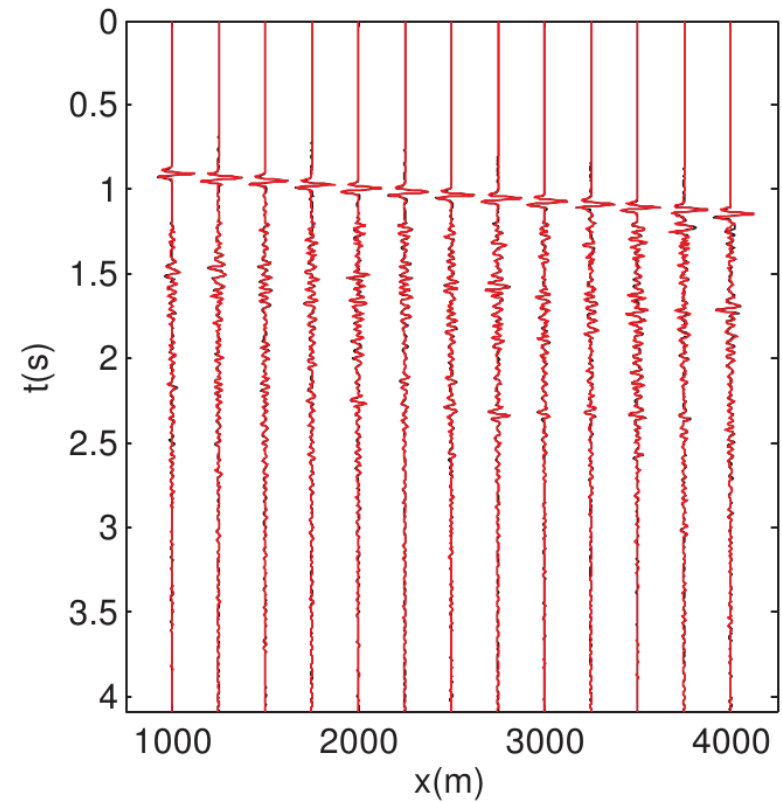


a)

a) The upgoing wavefield

red: the single-component approach

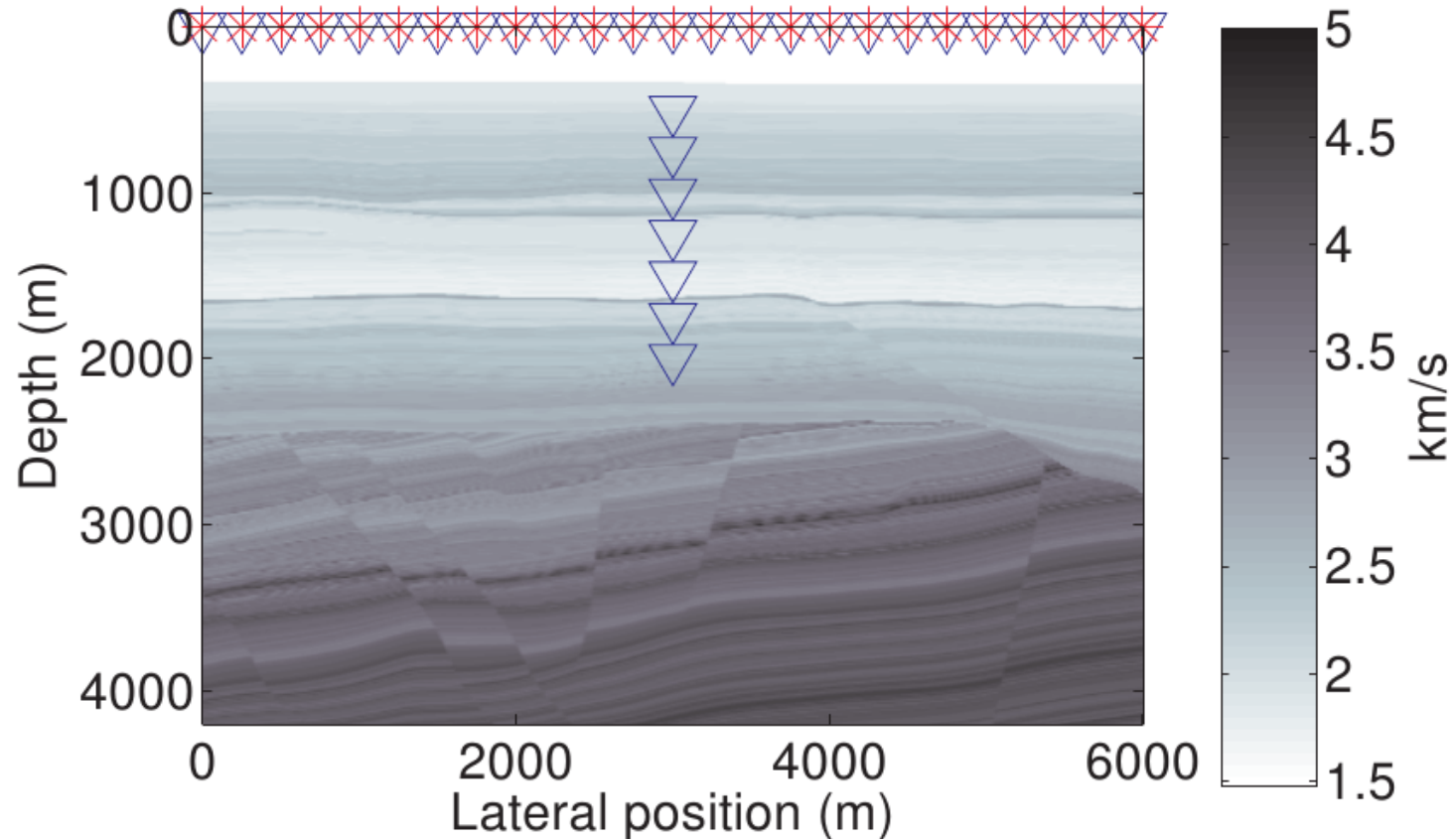
black: standard multi-component approach (p and vz).



b)

b) The downgoing wavefield

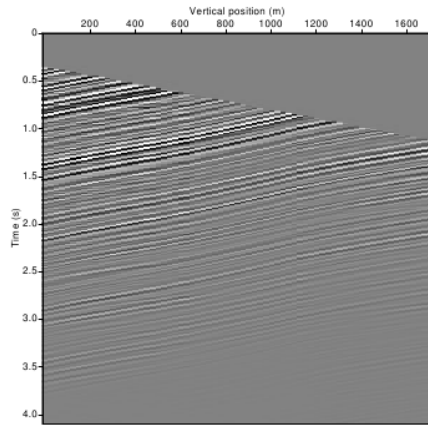
## Example 3: vertical borehole



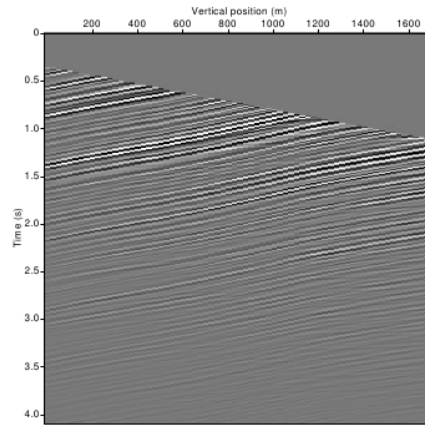
Surface:  $n_{src} = n_{rcv} = 241$ ;  $d_{src} = d_{rcv} = 25$  m;  $f_{max} = 55$  Hz.

Borehole:  $n_{rcv} = 69$ ;  $d_{zrcv} = 25$  m;  $z_{rcv} = [500, 1200]$  m; Ricker, 15 Hz.

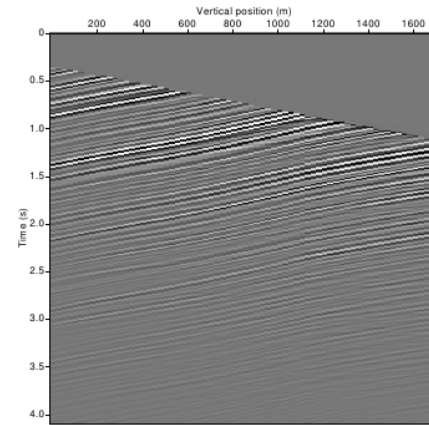
# Example 3: comparison of the up-down wavefields



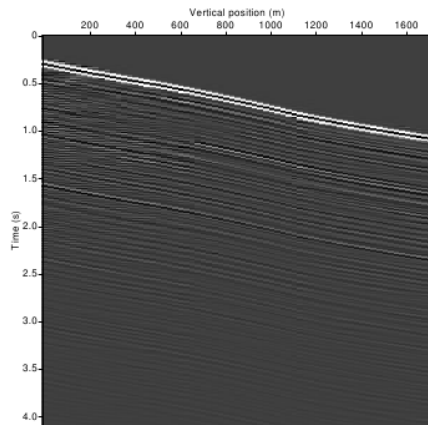
a)



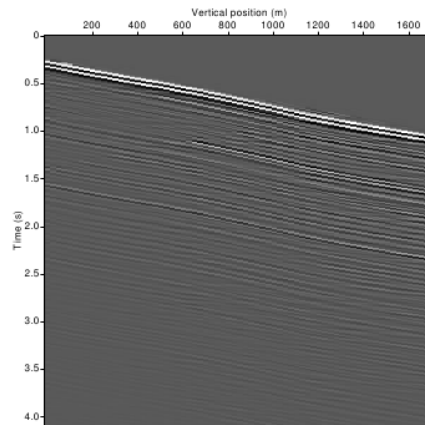
b)



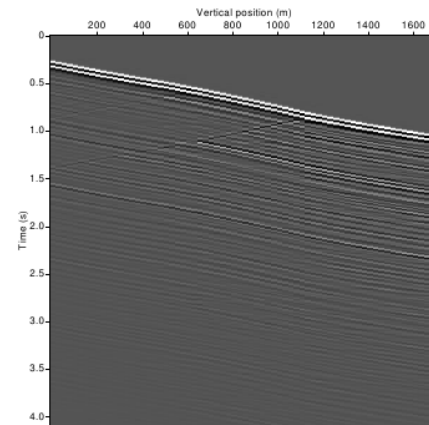
c)



d)



e)



f)

Single-component

single-component (with f-k dip filtering)

multi-component (PZ summation)

# Discussion

## Advantages:

- General lossless inhomogeneous medium, but smooth variation near the borehole;
- Wave-equation based, so all internal multiples are taken into account;
- No medium property information needed. No velocity error effect;
- Not limited to horizontal boreholes;
- Can be applied to a single borehole receiver, no receiver array need.

## Practical consideration:

- A good surface reflection response required: source wavelet deconvolution, surface multiple removal (SRME), a wide source and receiver coverage at the surface;
- Regularization of the source locations from the surface and borehole data;
- Limited illumination angle to steep reflectors compared to the actual decomposed borehole data.

# Conclusions

- A new single-component approach to retrieve the up-down wavefields in boreholes.
- Good agreement with those obtained by conventional decomposition methods.
- Although multi-component data are commonly available now, the possibility of retrieving the up-down wavefield using existing single-component data without any extra field cost is nevertheless attractive.

# Acknowledgements

- ROSE consortium at NTNU
- Jan Thorbecke at TUD for the open source modelling package
- Alexander Kritski at Statoil for the velocity model

# References

- Amundsen, L., and A. Reitan, 1995, Decomposition of multicomponent sea-floor data into upgoing and downgoing P- and S-waves: *Geophysics*, 60, 563–572.
- Barr, F. J., and J. I. Sanders, 1989, Attenuation of water-column reverberations using pressure and velocity detectors in a water-bottom cable: *SEG Technical Program Expanded Abstracts*, 653–656.
- Brogгинi, F., R. Snieder, and K. Wapenaar, 2012, Focusing the wavefield inside an unknown 1D medium: Beyond seismic interferometry: *Geophysics*, 77, A25 – A28.
- Embree, P., J. P. Burg, and M. M. Backus, 1963, Wide-band velocity filtering - The pie slice process: *Geophysics*, 28, 948–974.
- Moon, W., A. Carswell, R. Tang, and D. C., 1986, Radon transform wavefield separation for vertical seismic profiling data: *Geophysics*, 51, 940–947.
- Stewart, R. R., 1985, Median filtering: Review and a new F/K analogue design: *Journal of Canadian Society of Exploration Geophysicists*, 21, 54–63.
- Treitel, S., J. L. Shanks, and C. W. Frazier, 1967, Some aspects of fan filtering: *Geophysics*, 789-798.
- Wapenaar, K., J. Thorbecke, J. van der Neut, F. Brogгинi, E. Slob, and R. Snieder, 2014, Marchenko imaging: *Geophysics*, 79, WA39–WA57.
- Thorbecke, J. & Draganov, D., 2011. Finite-difference modeling experiments for seismic interferometry, *Geophysics*, 76(6), H1–H18.
- Wapenaar, K., Thorbecke, J., van der Neut, J., Brogгинi, F., Slob, E., & Snieder, R., 2014. Marchenko imaging, *Geophysics*, 79(3), WA39–WA57.

Thank you!